A PRELIMINARY MODEL OF THE EAST MESA HYDROTHERMAL SYSTEM

T. D. Riney, J. W. Pritchett, L. F. Rice
and S. K. Garg

Systems, Science and Software (S^3)
P. O. Box 1620, La Jolla, California 92038

ABSTRACT

A preliminary conceptual model of the East Mesa hydrothermal system is developed and a subregion selected for quantitative modeling. An axisymmetric model approximating the data available within the subregion is used together with a reservoir simulator to develop a computer model simulating the natural flow of heat and fluid mass within this geometric constraint. The axisymmetric calculations demonstrate that the balance between the convective and conductive modes of heat transport required to match the temperature and heat flow data implies a very low effective formation vertical permeability throughout the system.

The East Mesa hydrothermal system, lying in the southern Imperial Valley, is currently an area of active geothermal development. Fourteen geothermal wells (as of 1977) have been drilled within the KGRA. The geothermal reservoir lies below a depth of 2,000 feet and is separated from shallow groundwater aquifers by a clay cap of extremely low vertical permeability. We are presently developing an integrated computer model of the shallow and deep hydrothermal systems in the East Mesa region of the Imperial Valley which will be used to examine the response of the full hydrothermal system to large scale flow of geothermal fluid and associated heat transport. Of particular interest will be changes in the shallower groundwater system due to fluid mass and heat transport processes in the deeper geothermal system. The S^3 reservoir simulator MUSHRM is being used to synthesize the pertinent geothermal and geohydrological data base into a full three-dimensional model. Because of the incompleteness of the data base, the MUSHRM simulator has first been used in its two-dimensional mode of operation to perform a sequence of calculations to quantitatively investigate various aspects of a conceptual model of the East Mesa system and to examine the effects of uncertainties in the input data. This paper summarizes the results of a series of 2-D MUSHRM exploratory calculations performed for an axisymmetric approximation for the geothermal system.

Figure 1 presents a schematic of our conceptual model of the hydrological characteristics of the integrated East Mesa hydrothermal system.

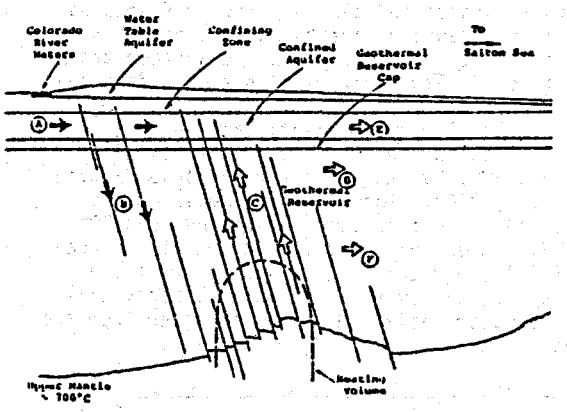

Fig. 1. Schematic of preliminary conceptual model of full East Mesa hydrothermal system and the subregion modeled in this project.

Seepage from the Colorado River and the unlined irrigation canal system is the principal source of the recharge water. Part of this recharge, (A), will flow into the shallow confined aquifer studied by Miller [1977]; part will flow down permeable faults, (B), since the recharge water is cooler (and denser) than the deeper fluid. The downward flowing water will be heated within some "heating volume". Some of the heated fluid mass will then convect upward along permeable faults, (C). Most of this upwelling fluid will likely either leak off laterally into the geothermal reservoir or be forced laterally by the relatively impermeable geothermal reservoir cap, (D), but some will leak across into the shallow confined aquifer, (E). Part of the fluid leaving the heating volume will also be pushed laterally, (F).

The parameters required to develop a computer simulation of the full hydrothermal system would include the three-dimensional distributions of temperature, water quality, rock thermal conductivity, porosity, permeability, etc. throughout the system. Knowledge of the natural flux of fluid mass and heat would also be required. Although the East Mesa system is one of the most extensively explored hydrothermal systems in the United States, sufficient data will probably never be available to model the complete system

represented schematically in Figure 1. Our effort is restricted to the depicted subregion which is centered on the geothermal anomaly and extends to a depth which includes the geothermal reservoir of interest for electrical power generation. It encompasses the region for which the bulk of the available geohydrologic data have been generated.

As indicated in the conceptual model, faults can act as conduits for rising geothermal fluids and descending cold groundwater. Three faults with no surface expression (Rex Fault, Babcock Fault and Combs-Hadley Fault) have been inferred. The three intersect near the center at the high heat flow region at East Mesa. Combs and Hadley [1977] hypothesize that the convective upwelling of hot fluid in an associated deep vertically fractured region is the cause of the measured abnormal surface heat flow. Figure 2 shows the surface traces of the three faults superposed on the surface heat flow contours at East Mesa. The contours are based on heat flow measurements made in shallow drill holes throughout the area. The raw data were reanalyzed by TRW and the results summarized by Pearson [1976]. The heat flow measurements extrapolate to surface temperatures between 80° and 90°F, rather than to the mean annual temperature of 73°F, probably due to poor thermal conductivity of the layer of unsaturated sandy soil above the water table and influx of water from the irrigation canals.

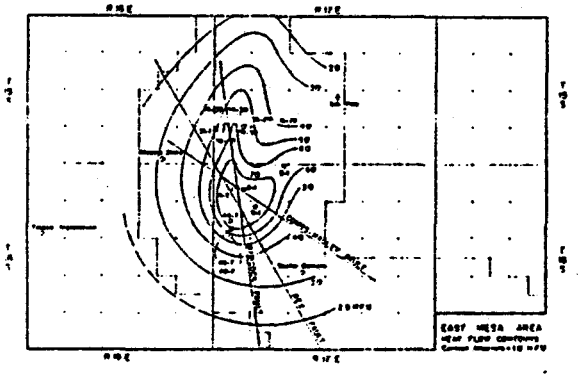

Fig. 2. Surface heat flow contours taken from TRW results [Pearson, 1976]. Locations of the four geothermal wells drilled subsequent to TRW analysis are denoted by □.

Strata in the East Mesa area, and throughout the central part of the Imperial Valley, are essentially horizontal. To provide a reference framework for constructing a model which includes the variations of the thermal and geohydrological characteristics of the region studied, we have divided the system into six horizontal layers (see Figure 3). From the earlier TRW analysis of the well logs from the geothermal and oil test wells in the region [Pearson, 1976], we have estimated the distribution of the formation porosity (ϕ) for the sand/shale sequence comprising each layer. The assumed temperature (T) distribution in the region is based on the approximate subsurface temperature contours at 1,000 foot depths constructed by TRW from well measurements.

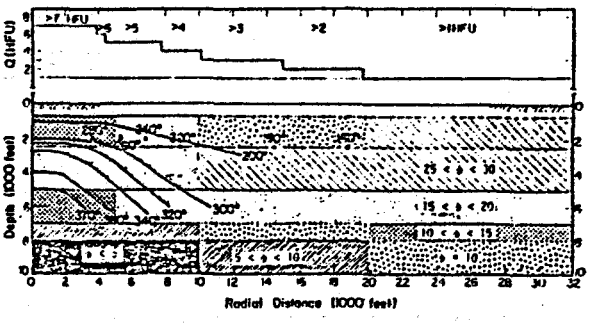

Fig. 3. Distribution of subsurface temperature (°F), surface heat flow, and formation porosity in idealized axisymmetric model. Axis of radial section is located near center of anomaly.

The axisymmetric approximation to the subsurface ϕ and T distributions are shown on the radial section presented in Figure 3; the axis of the section is considered to penetrate the center of the geothermal anomaly midway between Mesa wells 6-1 and 6-2. An axisymmetric approximation to the surface heat flow data (of Figure 2) is also shown.

The horizontal formation permeability (k_h) is assumed to be related to the porosity by a k_h - ϕ transform [Riney, et al., 1979]. The transform is calibrated by the LBL well test results [Witherspoon, et al., 1978; Narasimhan, et al., 1978], i.e., $k_h \sim 20$ md near the center of the geothermal reservoir. The corresponding distribution of k_h is defined by Figure 3 and the following transform values:

ϕ(%) :	0-5	5-10	10	10-15	15-20	20-25	25-30
k_h(md):	1	4	9	20	90	320	850

Since the interbedded shales and sands within each formation layer are predominantly horizontal, the vertical formation permeability (k_v) will be drastically restricted by nearly impermeable shales. Except for flow within vertical fractures, any net vertical flow will likely follow tortuous paths around the end of the interbedded shales, if such sand paths are in fact available. In the absence of any direct information, we will need to vary k_v parametrically in our model studies. That k_v is small near the center of the reservoir seems apparent from the fact that saline water is produced from the formation below 6,000 feet and dilute water from shallower depths [Hoagland and Elders, 1977].

Figure 4 compares the axial temperature profile with the data for the Mesa 6-2 well. the axisymmetric approximations to the data are

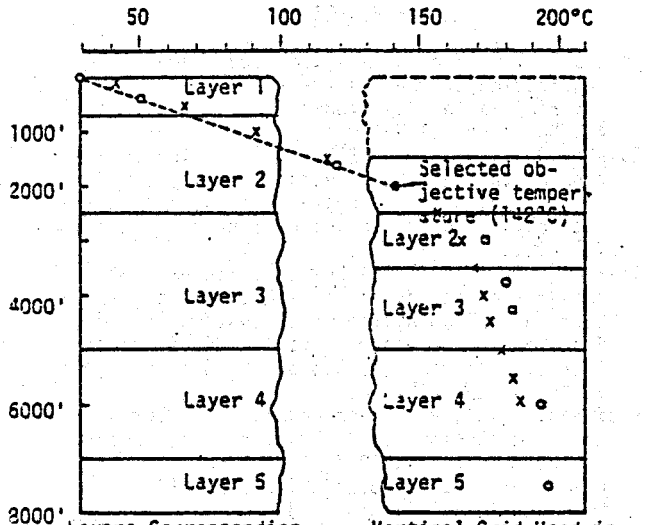

Fig. 4. Comparison of axial temperature-depth profile of axisymmetric model with the measured profile for the Mesa 6-2 well. The vertical dimensions of the finite difference grid used in the axisymmetric calculation is superposed.

reasonably good near the center of the anomaly. The model is incapable of representing the east-to-west variations in the sand content (and hence in ϕ) of the horizontal layers but radial variations are included in Figure 3 so that the general effect of lateral variations can be examined in the 2-D calculations. Any associated directionality of the fluid flow is necessarily ignored in the axisymmetric approximation; the cylindrical boundary conditions at the periphery of the model represent averaged conditions.

The axisymmetric model assumes that a cylindrically fractured region, in the vicinity of the intersection of the three faults shown in Figure 2, channels hot geothermal fluid from deep within the basement rock, through the otherwise nearly impermeable overlying shale-rich sedimentary sequence, and into the higher permeability sand-shale sequence that comprises the reservoir. Much of the hot fluid is shunted radially outward as it rises within the reservoir. The geothermal cap prevents any of the hot fluid from reaching the surface. We further assume that there is no fluid exchange across the bottom of the reservoir (bottom of layer 5) except the central convective influx. Then the total influx mass rate, $\dot{M}_c$, must be balanced by an equal net outward flow at the periphery of the subregion. The enthalpy of the fluid entering the reservoir less the enthalpy of the fluid leaving must be balanced by the surface heat flux in excess of the normal geothermal gradient. This leads to the approximation

$$\dot{M}_c = 16.9 \text{ kg/sec } (T_c = 469.26°K) .$$

In the numerical solution, the mass influx from the bottom boundary is represented by a mass source in the zone closest to the axis of symmetry (see Figure 5). Figure 5 shows the various boundary conditions used in the numerical model. The temperature distribution at the outer boundary (T_R), used to compute the fluid density and hence the prescribed hydrostatic pressure (P_R), was computed from the surface temperature and an effective thermal gradient. We note that thermal conduction dominates heat transfer above a depth of 2,500 feet (Figure 4); layer j = 1 lies in this regime and represents the lower part of the geothermal cap. The heat flux at the surface, Q_i, was modeled by a distributed volumetric heat sink in the top layer of the form

$$Q_i = A\,(T_{i1} - T_s)$$

where subscript i denotes the radial grid block, T_s is the surface temperature, T_{i1} is the computed temperature in the grid block (i,1) and A is a constant.

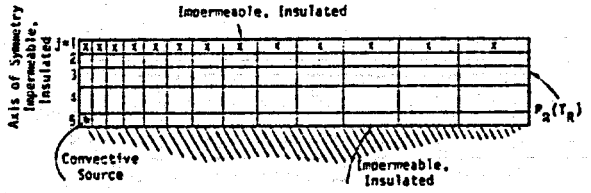

Fig. 5. Computational grid, internal sources/sinks, and boundary conditions. Heat flow through the top boundary is modeled by heat sinks in zones indicated by x.

A series of MUSHRM calculations employing the grid shown in Figure 5 were carried out to investigate the effects of permeability distribution upon the surface heat flux and subsurface temperature distribution. In an early calculation, we employed a formation porosity distribution which essentially duplicated that shown in Figure 3. The corresponding horizontal formation permeabilities (k_h) in each computational cell were calculated from the $\phi - k_h$ transform; the vertical formation permeability (k_v) in each computational cell in layers 2-5 was simply set equal to $k_h/3$. Since layer 1 acts as a geothermal cap, the value of $k_v = 10^{-3}$ md was used there. The calculated flow pattern exhibited a large convective loop accompanied by a temperature inversion in the reservoir. The convective loop is fed by two mechanisms (1) the rising hot fluid from the convective source which flows outward at the top and (2) the influx of colder (and denser) fluid from the outer boundary which flows inward at the bottom of the reservoir.

In attempts to interrupt the large convective loop, we tried various assumptions regarding permeabilities (e.g., reducing both horizontal and vertical permeabilities, larger vertical permeability in layer 1 at radii outside the hot spot to allow influx of cold water from top, introduction of a higher vertical permeability in the axial cells to simulate the penetration of the highly fractured cylindrical region into the reservoir), and convective source (e.g., increasing its strength). These calculations demonstrated that k_v must be drastically reduced to diminish the importance of the convective loop. It was found that a reduction in the vertical formation permeability to $k_v \sim 0.3 - 0.5$ md was required to establish the balance between conductive and convective heat transport. In one simulation, we employed porosity ϕ and horizontal permeability k_h corresponding to Figure 3; vertical permeability k_v was set equal to 0.5 md everywhere. Figure 6 shows the approximation to the steady-state solution obtained. The calculated temperatures and heat flux are in good agreement with the data (see Figure 3).

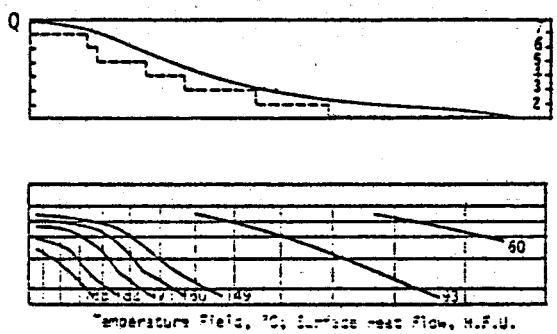

Fig. 6. Calculated steady-state temperature field. Simulated heat flow at surface is compared with values in axisymmetric model (Figure 3).

It is appropriate to point out here the nonuniqueness of the model. Riney, et al. [1979] describe a number of other simulations utilizing different porosity and k_h distributions which yield quite satisfactory agreement with the observed heat flow and temperature data. In the present case, however, there is sufficient information available that the range of parameters that give an adequate solution is reasonably limited. The conclusion that the effective formation vertical permeability in the East Mesa hydrothermal system is small appears to be on firm ground. This conclusion is in agreement with the model proposed by Hoagland and Elders [1977] for the evolution of the system. Goyal and Kassoy (see Goyal [1978]) have neglected vertical permeability altogether in their analytical studies of the geothermal reservoir.

ACKNOWLEDGMENTS

This work was sponsored by the U.S. Geological Survey's Geothermal Research Program under Contract No. 14-08-0001-16321

REFERENCES

Combs, J. and D. Hadley, 1977, Microearthquake investigation of the Mesa geothermal anomaly, Imperial Valley, California, Geophysics, Vol. 42, No. 1, pp. 17-33.

Hoagland, J. R. and W. A. Elders, 1977, The evolution of the East Mesa hydrothermal system, California, U.S.A., Proceedings, Second International Symposium on Water-Rock Interaction, Vol. III, pp. 127-136.

Miller, R. E., 1977, A Galerkin, finite-element analysis of steady-state flow and heat transport in shallow hydrothermal systems in the East Mesa area, Imperial Valley, California, Journal Research U.S. Geological Survey, Vol. 5, No. 4, pp. 417-508.

Narasimhan, T. N., R. C. Schroeder, C. B. Goranson and S. M. Benson, 1977, Results of reservoir engineering tests, 1977, East Mesa, California, Paper No. 7482, SPE, AIME, Houston, Texas, October 1-3.

Pearson, R. O., 1976, Planning and design of additional East Mesa geothermal test facilities (Phase IB), Vol. 1 of TRW final report of work performed under ERDA Contract No. E(04-3)-1140, October.

Riney, T. D., J. W. Pritchett, L. F. Rice and S. K. Garg, 1979, Integrated model of the shallow and deep hydrothermal systems in the East Mesa area, Imperial Valley, California, Interim Report, U.S.G.S. Contract No. 14-08-0001-16321, April.

Witherspoon, P. A., T. N. Narasimhan and D. G. McEdwards, 1978, Results of interference tests from two geothermal reservoirs, Journal of Petroleum Technology, Vol. 30, pp. 10-16.